

UNSTEADY-STATE DIFFUSION MODEL OF CRYOPRECIPITATE
FORMATION

V. N. Kukharenko and A. G. Kolgatin

UDC 536.422

This article describes a mathematical model for calculating cryoprecipitate thickness and density as desublimation parameters vary in a complex manner with time. Numerical results are given for the density distribution within a cryoprecipitate.

This paper proposes an unsteady-state mathematical model for cryoprecipitate formation on a chilled surface. The physical processes that take place in a cryoprecipitate layer are quite complex. They cannot be described in detail at the present level of research. Our model is therefore based on physical premises widely utilized in studies by various authors: 1) cryoprecipitate consolidation results from molecular diffusion of an impurity in the gas phase; 2) the impurity vapor is in thermodynamic equilibrium with the crystals within the cryoprecipitate, i.e., we assume ideal heat and mass transfer within the cryoprecipitate and an infinitesimal concentration relaxation time in the gas phase; 3) the portion of the impurity mass flux to the surface that is unable to diffuse into the cryoprecipitate goes to increase the layer thickness.

Thus, a mathematical model based on these assumptions was proposed in [1], and an analytic solution was obtained under the following assumptions: 1) absence of any density gradient within the cryoprecipitate; 2) a constant temperature gradient within it; 3) constancy of its surface temperature with time.

Absence of a density gradient within the cryoprecipitate was assumed in [2], and the temperature field over its thickness was described by a parabolic relation. The density and thickness were calculated by numerical methods.

The Soviet literature includes [3], in which the ice density was assumed to decrease from the chilled wall toward the precipitate surface by a linear rule.

The temperature and density distributions within the cryoprecipitate are calculated in our model by joint solution of the one-dimensional quasi-steady-state diffusion equation and the one-dimensional unsteady-state heat conduction equation.

As in [2], the expression for the impurity diffusion flux within the cryoprecipitate is defined as

$$J = -F_c \Psi \frac{\partial T_c}{\partial y}, \quad \text{where } \Psi = \left(1 - \frac{\rho_c}{\rho_{ice}} \right) \frac{\rho_m, c D}{1 - P_{im,c}/P_m} \left(\frac{dy_s}{dT} \right)_{T=T_c} \quad (1)$$

Here and in the sequel, the y-axis coincides with the outward normal to the cryoprecipitate surface. The diffusion equation can then be written in the form

$$\frac{\partial}{\partial y} \left(\Psi \frac{\partial T_c}{\partial y} \right) = - \frac{\Pi_c}{F_c} j_c \quad (2)$$

The heat conduction equation for the cryoprecipitate in the case under consideration has the form

$$F_c \frac{\partial}{\partial t} (c_c \rho_c T_c) = F_c \frac{\partial}{\partial y} \left(\lambda_c \frac{\partial T_c}{\partial y} \right) - r_{im} \Pi_c j_c \quad (3)$$

V. I. Lenin Khar'kov Polytechnic Institute. Translated from *Inzhenerno-fizicheskii Zhurnal*, Vol. 61, No. 3, pp. 447-451, September, 1991. Original article submitted July 17, 1990.

with the boundary conditions

$$\left(F_c \lambda_c \frac{\partial T_c}{\partial y} \right) \Big|_{y=0} = F_c \alpha_w (T_{c,w} - T_w) + (r_{im} J) \Big|_{y=0}, \quad (4)$$

$$\begin{aligned} \left(F_c \lambda_c \frac{\partial T_c}{\partial y} \right) \Big|_{y=h} &= F_c \alpha_s (T_m - T_{c,s}) + (r_{im} J) \Big|_{y=h} + \\ &+ r_{im} \beta \frac{M_{im} P_m}{0.5R(T_m + T_s)} \ln \left(\frac{P_m - P_{im,s}}{P_m - P_{im,f}} \right), \end{aligned} \quad (5)$$

where the relation for the impurity flow toward the surface conforms to the recommendations of [4]. Substituting the expressions for the impurity fluxes from (1)-(2) into Eq. (3) and boundary conditions (4)-(5) gives us the equation for determining the temperature field:

$$\frac{\partial}{\partial t} (C_c \rho_c T_c) = \frac{\partial}{\partial y} \left((\lambda_c + \Psi r_{im}) \frac{\partial T_c}{\partial y} \right) \quad (6)$$

with the boundary conditions

$$\left((\lambda_c + \Psi r_{im}) \frac{\partial T_c}{\partial y} \right) \Big|_{y=0} = \alpha_c (T_{c,w} - T_w), \quad (7)$$

$$\begin{aligned} \left((\lambda_c + \Psi r_{im}) \frac{\partial T_c}{\partial y} \right) \Big|_{y=h} &= \alpha_s (T_m - T_{c,s}) + \\ &+ r_{im} \beta \frac{M_{im} P_m}{0.5R(T_m + T_s)} \ln \left(\frac{P_m - P_{im,s}}{P_m - P_{im,f}} \right). \end{aligned} \quad (8)$$

That portion of the impurity which desublimates at the cryoprecipitate surface goes to increase its thickness [2]:

$$\rho_{c,s} \frac{dh}{dt} = \beta \frac{M_{im} P_m}{0.5R(T_m + T_s)} \ln \left(\frac{P_m - P_{im,s}}{P_m - P_{im,f}} \right) - \left(\Psi \frac{\partial T_c}{\partial y} \right) \Big|_{y=h}. \quad (9)$$

The impurity that desublimates within the cryoprecipitate increases its density:

$$\frac{\partial \rho_c}{\partial t} = - \frac{\Pi_c}{F_c} j_c = \frac{\partial}{\partial y} \left(\Psi \frac{\partial T_c}{\partial y} \right) \quad (10)$$

and

$$F_c \left(\frac{\partial}{\partial t} (\rho_c \Delta y) \right) \Big|_{y=0} = - J \Big|_{y=0}, \quad (11)$$

where Δy is the thickness of the ice film on the wall.

System of equations (6), (9), (10), and (11) with boundary conditions (7)-(8) must be supplemented by uniqueness conditions: 1) the equations of state for the gas mixture and the saturated vapor over a crystal; 2) the relationship for computing the heat and mass transfer coefficients; 3) the thermophysical properties of the atmosphere.

The resultant system of differential equations is solved by the finite difference method, utilizing an implicit four-point scheme and process separation.

The mathematical model was tested with the experimental data of [5] on the freezing out of carbon dioxide from a carbon dioxide-nitrogen mixture onto a chilled plate, under the following conditions:

1. The equation of state was that for an ideal gas.
2. The saturated vapor pressure over a crystal was determined from the relationships

[6]

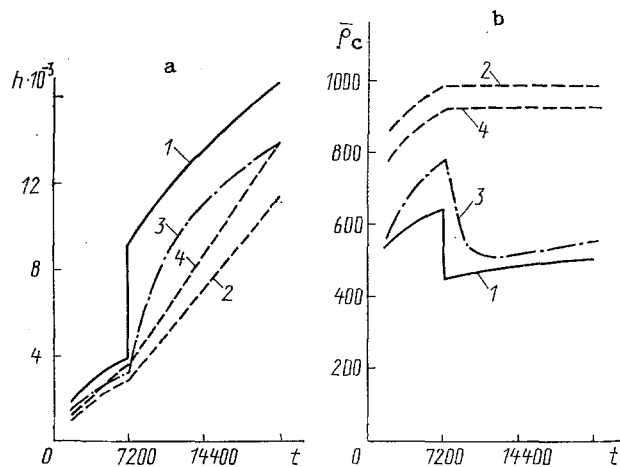


Fig. 1. Increase in cryogenic thickness (a) and change in average density (b) with time. 1) From empirical relationships of [8]; 2) calculations made with model having linear approximation of temperature profile within cryoprecipitate and neglecting density gradient; 3) calculations made with our model; 4) calculations made with model of [2]. Wall temperature was lowered from 148 to 98 K after 7200 sec.

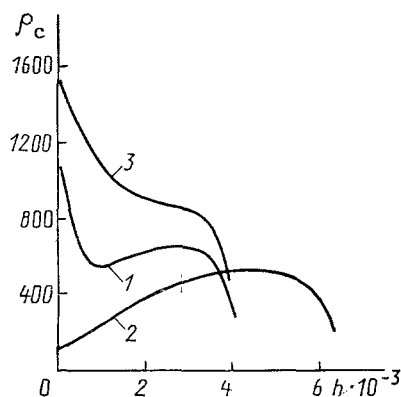


Fig. 2. Characteristic density distribution within cryoprecipitate at mixture temperature of: 1) 140; 2) 110; 3) 155 K.

$$P_{s1} = 133.322 \cdot 10^{(-1368/T + 9.915)} \text{ when } T \geq 140 \text{ K};$$

$$P_{s1} = 133.322 \cdot 10^{(-1275.6/T + 0.006837T + 8.307)} \text{ when } T < 140 \text{ K.}$$

(12)

3. The heat and mass transfer coefficients were calculated from the empirical relationships [7]

$$Nu = 0.273 Re^{0.6} Pr^{0.37},$$

(13)

$$Nu_D = 0.288 Re^{0.6} Pr_D^{0.37}.$$

(14)

4. The effective coefficient of thermal conductivity was determined with the generalized relationship obtained for a porous substance in [8] by analysis of structural models. The proposed relation assures an error of about 15% for a porosity of 20-80%. The relationship for the case under consideration took the form

$$\lambda_c = \lambda_{ice} \left(1 + \left(5.5 \frac{\lambda_m}{\lambda_{ice}} - 2.42 \right) \left(1 - \frac{\rho_c}{\rho_{ice}} \right) \right) \text{ when } \frac{\rho_c}{\rho_{ice}} > 0.8, \quad (15)$$

$$\lambda_c = \lambda_{ice} \left(-0.188 + 0.88 \frac{\rho_c}{\rho_{ice}} + 1.1 \frac{\lambda_m}{\lambda_{ice}} \right) \text{ when } 0.4 \leq \frac{\rho_c}{\rho_{ice}} \leq 0.8, \quad (16)$$

$$\lambda_c = \lambda_{ice} \left(-0.012 + 0.44 \frac{\rho_c}{\rho_{ice}} + 1.1 \frac{\lambda_m}{\lambda_{ice}} \right) \text{ when } \frac{\rho_c}{\rho_{ice}} < 0.4. \quad (17)$$

The dependence of thermal conductivity on temperature for crystalline carbon dioxide was obtained by approximating the data of [9] (the error was no more than 5%):

$$\lambda_{ice} = 0.6 (153/T_c). \quad (18)$$

Use of theoretical relationships (15)-(18) in place of the experimental data of [7] altered the results yielded by the cryoprecipitate thickness and density calculations by no more than 5%.

5. The diffusion coefficient was determined as a function of temperature by the method of [10].

6. It is necessary to specify the cryoprecipitate density at the surface in order to make calculations with the proposed model. There are few experimental data on this parameter, and we therefore made preliminary computations with different densities for a broad range of process parameters. It was established that, for average cryoprecipitate densities of more than $0.2\rho_{ice}$, variation of the initial density from $0.2\bar{\rho}_c$ to $0.9\bar{\rho}_c$ changed the calculated values by no more than 5%. We assumed $\rho_s = 0.5\bar{\rho}_c$ for the calculations.

The initial cryoprecipitate density and thickness were assumed to be $\rho_c(0) = 100 \text{ kg/m}^3$ and $h(0) = 10^{-5} \text{ m}$. A further decrease in these parameters did not lead to any perceptible change in the calculated results but required a larger amount of computer time.

The computational results for various models were compared with the experimental data of [5] under the following conditions: a mixture temperature of 193 K, wall temperatures of 148 and 98 K, mixture flow velocities of 0.5 m/sec, and an impurity partial pressure of 4350 Pa (Fig. 1). When the wall temperature was constant, the calculated results were in qualitative agreement with the experimental data. A sharp change in wall temperature (as is characteristic when cryogenic equipment departs from normal operating conditions) causes substantial nonuniformity of cryoprecipitate density, which should be manifested in a smooth transition in the corresponding experimental curve. Of the three models considered, only ours provided a qualitatively correct description of this process.

Figure 2 shows the density distribution over the cryoprecipitate thickness for different desublimation conditions. Curve 1 was characteristic of moderate supercooling. The increased cryoprecipitate density near the wall was responsible for the lengthy duration of the process and the high temperature gradient during its initial stage. The maximum near the cryoprecipitate surface was produced by the high diffusion flux densities resulting from the high temperatures (saturated vapor pressure and impurity diffusion coefficient). The saturated vapor pressure of the impurity was small at low wall temperatures (curve 2), so that the impurity partial pressure gradient was small even in the presence of large temperature gradients and diffusion was impeded. There was no cryoprecipitate density maximum near the chilled wall in this case. No density maximum occurred near the cryoprecipitate surface when degree of supercooling was low (curve 3). Qualitatively similar density profiles for cryoprecipitates were observed in [11, 12].

CONCLUSIONS

1. An unsteady-state mathematical model and a computation algorithm have been proposed for cryoprecipitate formation, with allowance for the nonuniformity of density over the cryoprecipitate thickness as desublimation conditions undergo complex variation with time. Relationships have been derived for determining effective cryoprecipitate thermal conductivity. Satisfactory agreement was obtained with experimental data.

2. Calculation of the density distribution within a cryoprecipitate has shown that a density maximum occurs at the wall or near the cryoprecipitate surface, depending on process conditions. The two maxima can be simultaneously present, or the density distribution can be almost uniform. These calculations make it possible to explain the discrepancy in the results of different experimental studies of the density distribution within cryoprecipitates.

NOTATION

c) Specific heat capacity; D) impurity diffusion coefficient; F) cross-sectional area; h) cryoprecipitate thickness; j) density of impurity flux from solid crystals into gas mixture; J) impurity flux; Nu) Nusselt number; P) pressure; Pr) Prandtl number; r) heat of sublimation; Re) Reynolds number; t) time; T) temperature; y) coordinate on axis coinciding with outward normal to wall; α) heat transfer coefficient; β) mass transfer coefficient; γ) impurity mass fraction; λ) coefficient of thermal conductivity; Π) heat and mass transfer perimeter; ρ) density. Indices: D) diffusion; c) cryoprecipitate; sat saturation; f) flux; im) impurity; w) wall; m) mixture; ice) crystals; s) cryoprecipitate surface. An overscore indicates averaging over coordinate.

LITERATURE CITED

1. P. L. T. Brian, R. C. Reid, and I. Brazinsky, *Cryogenic Technol.*, 5, 205-212 (1969).
2. D. W. Jones and J. D. Parker, *J. Heat Trans. ASME.*, 97, 255-300 (May, 1975).
3. V. A. Varivoda, *Kholod. Tekh. Tekhnol.*, No. 47, 85-92 (1988).
4. *Handbook of Heat Exchangers* [in Russian], Vol. 1, Moscow (1987).
5. V. N. Shelkunov, N. Z. Rudenko, and Yu. V. Shostak, *Kholod. Tekh.*, No. 5, 21-26 (1986).
6. M. P. Malkov (ed.), *Handbook of Physicotechnical Principles of Cryogenics* [in Russian], Moscow (1973).
7. N. Z. Rudenko, "Desublimation of carbon dioxide and water vapor from gas mixtures," Author's abstract of candidate's dissertation, Khar'kov (1988).
8. V. V. Dyablo, S. D. Getel'baum, and V. B. Batal'skii, *Izv. Vyssh. Uchebn. Zaved., Énergetika*, No. 12, 78-80 (1988).
9. B. I. Verkin, B. F. Getmanets, and P. S. Mikhal'chenko, *Thermophysics of High-Temperature Sublimational Cooling* [in Russian], Kiev (1980).
10. R. Reid, J. Prausnitz, and T. Sherwood, *Properties of Gases and Liquids*, McGraw-Hill, N.Y. (1968).
11. G. J. Trammel, D. C. Little, and E. M. Killgore, *ASHRAE J.*, No. 7, 42-47 (1968).
12. C. J. Cremers, O. J. Hahn, and J. H. Skorupski, *Adv. Cryog. Eng.* 23, 371-376 (1978).